The Impact of Surface Area on the Radiative Thermal Behavior of Embedded Systems

Karel De Vogeleer, Pierre Jouvelot, and Gerard Memmi

Abstract—A new global analytical model of the heat dissipation process that occurs in passively-cooled embedded systems is introduced, and we explicit under what circumstances the traditional assumption that exponential cooling laws apply in such context is valid. Since the power consumption and reliability of microprocessors are highly dependent on temperature, management units must be able to rely upon accurate thermal models. Exponential cooling models are justified for actively-cooled microprocessors. For passively cooled processors however, as frequently found in embedded systems such as mobile devices, an exponential law may not be theoretically justified. Here, we analyzed the tractability of the cooling law for a passively cooled body, subject to radiative and convective cooling. Focusing then on embedded microprocessors, we compare the performance difference between our new passive cooling law and the conventionally-used exponential one. We show that, for isothermal cooling surfaces of the order of $1\,\mathrm{dm}^2$ or greater, the radiative cooling effect may become comparable to the convective cooling one. Otherwise for surfaces below $1\,\mathrm{dm}^2$, we show that the differences between the exact solution and the exponential cooling law are negligible. In the absence of accurate temperature measurements, an exponential cooling law is shown to be accurate enough for small-sized SoC systems that require low processing overhead.

Index Terms—Passive cooling, mobile embedded systems, cooling law approximation, radiative cooling, SoC, cooling laws.

✦

1 INTRODUCTION

G IVEN the crucial aspect of energy optimization in embedded and mobile systems, even a tiny amount of energy gained via a better understanding of thermal effects may have significant business and ecological impacts. Temperature is an important factor influencing energy consumption of microprocessors while executing programs. Understanding and accurately modeling this relationship may bear impact beyond optimized system operation management. This point is particularly acute for any system running on electrical battery such as mobile devices or sensors which participate in the Internet of Things (IoT).

Moreover, temperature and its variations affect the reliability of circuits. Thermal gradients that occur both in space and time, induced by the variability in microprocessor load and operations, generate thermal cycles that have an adverse affect on the failure rate of systems [1]. A $10°C$ to $15°C$ temperature increase may halve a microprocessor's lifetime [2]. The International Technology Roadmap for Semiconductors (ITRS) even states that processor costs and performance specifications may be limited by the lifetime reliability and is of primary concern in the microprocessor's design phase [3]. Since power consumption increases exponentially with increasing silicon temperature [4], thermal management techniques are required to avoid self-destruction, to increase the Mean Time To Failure (MTTF) and minimize power consumption. Such thermal techniques may be used at the system design phase or can be deployed dynamically at run time by Thermal Management Units

(TMUs) and Dynamic Thermal Management (DTM) systems. A plethora of thermal control methods for microprocessors exist [5] and show trade-offs between temperature profile, frequency settings, power consumption and implementation complexity.

Thermal management methods often incorporate a model describing the temporal thermal behavior of the microprocessor. Exponential-based models are popular, and scientifically sound for systems without internal heat generation and subject to active cooling, e.g., forced air or water cooling. It has also been shown that an exponential law may be a good approximation when simulating the conduction of heat, under very specific circumstances: when the average system temperature is not too large and the system conducts heat much faster than it gains heat from its surroundings [6]. However, passively cooled systems, as frequently found in embedded devices particularly mobile devices, but also flats screen TVs etc., are not always forcibly cooled. These are subject to the same physical laws for dissipating their heat to the environment, but rely on different aspects of the heat dissipation process.

In this paper, we develop an accurate analytical solution to the problem of modeling the passive cooling of embedded systems. It is important to understand the difference between an exponential cooling law and the cooling law of passively cooled devices since, in the literature, the radiative cooling aspect is frequently neglected. We believe that this is because it is considered a secondary order factor and because of its non-linear nature, which poses problems in mathematical derivations and simulations. In the case of active cooling, convective heat transfer dominates the other heat transfer modes whereas, for passive cooling, radiation may become equally important, sometimes even more important, and may dominate the convective heat

- *K. De Vogeleer and Gerard Memmi are with TELECOM ParisTech – INFRES – CNRS LTCI - UMR 5141 – Paris, France, Email: {karel.devogeleer,gerard.memmi}@telecom-paristech.fr*
- *Pierre Jouvelot is with MINES ParisTech, PSL Research University, France. Email: pierre.jouvelot@mines-paristech.fr*

transfer mode. When radiation cannot be neglected, the transient thermal behavior of the system will deviate from an exponential cooling law. In this paper we analyze under which circumstances the radiation is significant enough for it not to be neglected. We show that the size of the cooling surface plays an important role in this question. In particular, in cases where the cooling surface of the device is large ($> 1\,\mathrm{dm}^2$), the difference between the exponential and passive cooling laws is significant. Based on the passive cooling law's complex formulation and in the absence of accurate temperature measurement samples, our work therefore suggests that an exponential cooling law is accurate enough for SoC applications and systems that require low processing overhead.

We compare the active and passive cooling of a microprocessor in the context of a mobile embedded system, i.e., a low-power processor subject to internal heating generation and cooling. The main contributions of this paper are:

- the accurate analytical solution for the problem of (passive) cooling of a microprocessor subject to radiation, convection, and internal heat generation;
- approximations to the exact analytical solution for use in practical applications;
- actionable rules-of-thumb to assess when passive cooling becomes non-negligible compared to active cooling in embedded systems;

The rest of the document is developed as follows. Section 2 highlights the use of cooling laws in existing research related to thermal management units. Section 3 develops the exact cooling law for microprocessors subject to passive cooling; this law is also validated via finite-element simulations and approximations are analyzed. Besides, the impact of active cooling of microprocessors is also discussed. Section 4 studies the performance difference between the exponential cooling law and the passive cooling law. We conclude in Section 5 with a summary and give directions for future research.

2 RADIATIVE COOLING IN EXISTING THERMAL MANAGEMENT TECHNIQUES

Thermal management techniques for microprocessors have been devised to control their heat dissipation. Excessive heat dissipation may have adverse effects on performance, and the short term and long term failure rate of the microprocessor. Basic run-time thermal management techniques can be rudimentary, such as clock gating. Yet, if service continuation is needed, more advanced thermal techniques are required. Thermal-aware design of microprocessors can also be effective to minimize peak and average heat dissipation during run time. The challenge here, however, lies in decision making based on incomplete design and run-time details.

To get a current perspective on how such issues are addressed in the literature, we surveyed top computer architecture and Very-Large-Scale Integration (VLSI) conferences for papers devoted to TMUs, DTMs and temperature-aware design methods based on heat transfer theory. The conferences surveyed are ISCA, MICRO, ASPLOS, HPCA, PACT, ISLPED, ICCAD, DAC, DATE, ASP-DAC from 2010

to 2014. We identified 35 papers focusing on the thermal optimization of microprocessors using heat transfer models. 90% of these papers base their results solely upon simulation or numerical analysis; the remaining ones use either actual measurements or a combination of simulation and measurements to make their point. Beside custom thermal simulators and models, non-commercial and open-source thermal simulators are mostly used: these are based on finite-element methodologies. Commercial applications such as COMSOL Multiphysics®, Autodesk Simulation CFD or FLoTHERM®, which support the radiative heat transfer mode, are not used in the selected papers. About 40% of the selected papers deploy Hotspot for their thermal simulations. Hotspot [7] is a self-proclaimed accurate and fast thermal model designed for microprocessor architectural analysis, e.g., floor planning. The basic setup of Hotspot includes active cooling via a heat sink. No passive cooling capabilities are available in Hotspot. Other experimental simulators, such as LightSim [8], CONTILTS [9], ISAC [10] and PowerBlurr [11], also allow for thermal analysis of microprocessors, but are less popular and none support radiative cooling. In most of the simulations, the temperature at steady state and transient temperatures are available, where the steady-state case is much faster to compute than the transient behavior.

It is worthwhile to ponder upon why no non-commercial simulators support radiative cooling. One reason could be that the non-linear behavior of radiation is not easy to handle in mathematical formulations and advanced finite element techniques need to be employed in numerical simulations. Also it is not always clear to what extent radiation actually affects the thermal behavior of semiconductors. As a result, given the lack of handling of passive cooling in most simulators, it is not surprising that passive cooling has not gotten much attention in the thermal management research community. In fact, we only found one paper [12], about 3D integrated circuits which mentions that radiation may influences the thermal behavior of microprocessors; yet in this work no further reference to radiation is found. Nevertheless, 30% of the papers we surveyed claim that their research is applicable to mobile embedded systems, a situation in which passive cooling is usually of the essence.

Beside generic thermal microprocessor simulators, dedicated embedded system thermal simulators were also developed. Therminator [13], for example, is a thermal simulator designed to simulate heat dissipation in smartphones. Finite element methodologies are used to compute the heat propagation through an arbitrary smartphone configuration, which may include a printed circuit board (PCB), battery, case, display etc. The authors show that their dedicated thermal simulator produces results that are close to what commercial computational fluid dynamics (CFD) software would calculate. Therminator takes the convective and conduction heat transfer modes into account. Heat loss via radiation, however, is not implemented in their thermal simulator. Luo et al. [14] analyzed the issue of thermal management on mobile phones based on numerical simulation and basic thermal models. The authors came up with design proposals on how to improve the thermal management of mobile phones by studying the steady-state behavior of the system. Even though radiation is mentioned

in the introduction including formulations, radiation is not present in their stead-state analysis. Gurrum et al. [15] decomposed, just as Luo et al. [14], a hand-held device in multiple subparts with different physical properties and analyzed its thermal behavior. Radiation, however, did not come to their attention.

From our literature survey we conclude that the numerical tools used for thermal behavior of embedded systems can be classified into three categories. First, we have the general-purpose CFD software, which is able to simulate arbitrary systems including all modes of heat transfer. These systems require the most efforts to produce interesting results. The second class corresponds to dedicated embedded system simulators. We have observed that the designers of the simulators are aware of surface radiation but they do not provide support in their simulators. And last, which are the most popular, are the generic microprocessor thermal simulators. We have not seen any of these microprocessor simulators supporting the radiative heat transfer mode. This provided us with a strong motivation for our work, which strives to understand the possible impact of radiation on the transient and steady-state thermal behaviors of microprocessors in the context of embedded systems.

3 COOLING LAWS

The exponential cooling law is the most widely used cooling law to model the thermal behavior of microprocessors, as shown by our literature survey. The rationale behind an exponential law is based on temperature traces of forcibly cooled microprocessors, which indeed show clear exponential behavior [14], [15]. One may attribute the exponential curve to Newton's law of cooling. However, the presence of internal heat generation, which renders the direct applicability of Newton's law of cooling irrelevant for microprocessors, should not be forgotten. In the sequel we show however that Newton's law of cooling extended with internal heat generation also yields an exponential cooling law. For passively cooled microprocessors, the radiative heat transfer mode, beside natural convection, also needs to be taken into account.

In this section, after a brief overview of basic heat transfer principles [16], we develop the cooling law for an actively cooled body. We then extend this model with radiative cooling to obtain our first contribution, a representative model for passively cooled systems.

3.1 Basics of Heat Transfer

Heat transfer happens via a combination of the three fundamental modes: *convection*, *conduction*, and *radiation*. Each of these modes follows its respective law. In the sequel we assume an isothermal body that cools via convection and radiation. Isothermal conditions may be approximated if the body heats up uniformly, or if the internal heat conduction happens considerably faster than the heat loss of the body to the environment. Therefore we won't discuss conduction in detail.

A solid body immersed in a moving fluid, e.g, air or water, is subject to energy exchange if the temperatures of the body and the moving fluid differ. Energy is *convected* from or to the body if the moving fluid has a different temperature from the body. The energy transfer rate q [W] between the moving fluid and the surface of the body is formally known as *Newton's law of cooling*:

$$q = C\frac{dT}{dt} = h_{ac}S(T_m - T), \qquad (1)$$

where T_m is the temperature of the moving fluid (environment), S, the cooling surface area of the body, and h_{ac}, the *convective heat transfer coefficient* [W/(m^2·K)].

Radiative heat transfer happens through exchange of electromagnetic waves, possible through both vacuum and transparent media. Stefan-Boltzmann's law states that the power radiated from a *blackbody* is proportional to its temperature. A *blackbody* is a body that absorbs all incident radiation. In particular, Stefan-Boltzmann's law states that the radiative heat transfer rate q is proportional to the blackbody's temperature to the 4th power:

$$q = \epsilon\sigma ST^4, \qquad (2)$$

where $\epsilon \in [0, 1]$ is the *emissivity* of a gray body's surface (dimensionless), and σ is the Boltzmann constant 5.6697×10^{-8} [W/(m^2·K^4)]. A *gray body* is a body that reflects a certain amount of the incident radiation. The emission and absorption of a gray body can be well represented by a blackbody's behavior scaled by its emissivity: $0 < \epsilon \leq 1$. In practical situations the total heat loss of a body via radiation is equal the emitted radiation minus the absorbed radiation:

$$q = \epsilon\sigma S(T_a^4 - T^4), \qquad (3)$$

where T_a is the radiation temperature of the environment. Here we implicitly assumed that the environment has the same emissivity as the body itself.

The total heat transfer from a body happens via the combination of the basic heat transfer modes. Beside, a body may also produce heat $H(\cdot)$ [W] which is referred to as *internal heat generation*. The internal heat generation is a function of space, time, temperature or others. In the sequel we will assume that the internal heat generation is homogeneously present throughout the entire body.

3.2 Active Cooling: the Newtonian Approach

Newton's law of cooling states that the temperature rate of change of an object is proportional to the difference between the ambient temperature and the object's temperature. Thermal Management Units (TMUs) and Dynamic Thermal Managements (DTMs) often assume the system to cool down following Newton's law of cooling. Accordingly it is implicitly assumed that the system's power consumption as a result also exhibits exponential behavior over time, comparable to an RC network. Such assumptions are frequently found in thermal management systems [1], [17], [18], [19], [20], [21], [22]. For actively cooled systems, i.e., cooled using forced convection (such as computer fans or water cooling), an exponential assumption is a good approximation when radiative and conductive cooling may be neglected, as we explain now.

Assume that for such systems the stored energy is approximated by the sum of the heat transfer induced by *con-*

vectional cooling: $h_{ac}S(T_m - T)$, and an *internal heat generation* (ihg), which we deem linear as a first-order approximation:

$$
\begin{aligned}
C\frac{dT}{dt} &= \text{convection} + \text{internal heat generation} \\
&= hS(T_m - T) + (\eta_1 T + \eta_0).
\end{aligned} \tag{4}
$$

where C is the body's heat capacity and T_m the ambient temperature. Note that, if the active cooling system consists of a fan and heat sink, then h_{ac} depends upon the dimensions of the heat sink or body surface area, and the revolutions per minute (rpm) of the fan. Moreover, η_1 and η_0 are also dependant on the operating frequency of the microprocessor and the load on the system. Similar to Weissel and Bellosa's [23] work, one gets, from Equation 4:

$$
T - \frac{\eta_0 + h_{ac}ST_m}{h_{ac}S - \eta_1} = c_0 e^{-\frac{(h_{ac}S - \eta_1)}{C}t}, \tag{5}
$$

while imposing the initial condition at $t = 0$: $T(0) = T_0$. Therefore $c_0 = T_0 - \frac{\eta_0 + h_{ac}ST_m}{h_{ac}S - \eta_1}$, and thence

$$
T_{ac}(t) = \frac{\eta_0 + h_{ac}ST_m}{h_{ac}S - \eta_1} + \left(T_0 - \frac{\eta_0 + h_{ac}ST_m}{h_{ac}S - \eta_1} \right) e^{-\frac{(h_{ac}S - \eta_1)}{C}t}. \tag{6}
$$

It is clear that such a system is only stable if the cooling process with constant h_{ac} convects heat away from the system faster than the system is generating internal heat. The system is stable if there exists an equilibrium temperature T_e for the system, which is equivalent to saying that

$$
0 = h_{ac}S(T_a - T_e) + (\eta_1 T_e + \eta_0) \Rightarrow h_{ac} = \frac{\eta_1 T_e + \eta_0}{S(T_e - T_a)}, \tag{7}
$$

where all constants $\{T_e, T_m, \eta_1, \eta_0\} \in \mathbb{R}^+$. We can state, given that h_{ac} must be positive, that $T_e > T_m$. We can also conclude from Equation 6 that h_{ac} is always larger than η_1/S. If $h_{ac} < \eta_1/S$, the exponent in Equation 6 would go to infinity over time. In practical applications the value of h_{ac} must be dimensioned properly such that the system's T_e stays below the maximum operation temperature.

Not surprisingly, Newtonian cooling with linear internal heat generation yields again an exponential relationship between temperature and time. Consequently, the power P consumed by the system, which is an affine transformation of temperature ($P = \eta_1 T + \eta_0$), will also exhibit exponential behavior. An exponential model for actively cooled systems with linear (or constant, $\eta_1 = 0$) internal heat generation is therefore a valid approximation. The exponential assumption is however not quite the same as assuming simple Newtonian cooling, as the coefficients in both models are different, mainly due to the presence of the internal heat generation. In the case of the presence of internal heat generation the equilibrium temperature T_e of the system will be larger than the ambient temperature, see Equation 6 if $t \to \infty$.

3.3 Passive Cooling via Radiation, (Natural) Convection and subject to Internal Heat Generation

We now extend the previous model to better fit passively cooled embedded systems. Bodies that are not actively cooled must indeed rely on passive cooling to attain a temperature equilibrium state. Passive cooling mechanisms include radiation, and also convection. Note though that convection, in this case, may be considerably smaller than when the system is actively cooled. The convection arising here may be originating from buoyancy forces, or natural movement of air, e.g., wind. In the case of buoyancy forces, sometimes the convection is referred to as *natural convection* as the movement of air is not enforced on the system.

Assume an isothermal body subject to radiative cooling and convection with internal heat generation. The temperature change of such an object at any given point in time is equal to the heat absorbed from the environment, plus the internal heat generation, minus the heat released to the environment. Absorption of heat happens via radiation whereas the release of heat is happening both via radiation and convection. The temperature change of such a system, with internal heat generation (ihg), can be represented by the following equation:

$$
\begin{aligned}
C\frac{dT}{dt} &= \text{radiation} + \text{convection} + \text{ihg} \\
&= \epsilon\sigma S(T_a^4 - T^4) + hS(T_a - T) + (\eta_1 T + \eta_0) \tag{8}
\end{aligned}
$$

where ϵ is the emissivity of the body, and σ is the Boltzmann constant. Here it is assumed that the internal heat generation is linearly dependent on the temperature of the body: $H(T) = \eta_1 T + \eta_0$. Yet, higher order polynomials (up to the 3th order) can be used as well for the following derivation to hold (as we show in Appendix A). Also, T_m is presumed to be equal to T_a.

By rearranging Equation 8 we obtain:

$$
\frac{dT}{dt} = \frac{1}{C}\{-\epsilon\sigma ST^4 + (\eta_1 - hS)T + (\eta_0 + S[hT_a + \epsilon\sigma T_a^4])\}. \tag{9}
$$

Here, the right-hand side is a 4th-order polynomial.

The derivation provided in Appendix B shows that the exact solution to the problem of cooling of a body subject to radiation, convection, and internal heat generation is given by Equation 10.

$$
\begin{aligned}
t = -\frac{1}{\kappa_4}\Big(&A\ln|T - \omega_1| + B\ln|T - \omega_2| + \frac{C}{2}\ln|(T - \alpha)^2 \\
&+ \beta^2| + \frac{\alpha C - D}{\beta}\arctan\left(\frac{T - \alpha}{\beta}\right) + c_o \Big), \tag{10}
\end{aligned}
$$

Here c_o must satisfy the initial conditions $t(T_0) = 0$, if $t(T)$ denotes the right-hand side expression in Formula 10 :

$$
\begin{aligned}
c_o = &-A\ln|T_0 - \omega_1| - \frac{C}{2}\ln|(T_0 - \alpha)^2 + \beta^2| \\
&-B\ln|T_0 - \omega_2| - \frac{\alpha C + D}{\beta}\arctan\left(\frac{T_0 - \alpha}{\beta}\right) \tag{11}
\end{aligned}
$$

the ω_* are the roots of the 4th-order polynomial given in Equation 9 ($\omega_{1,2}$ are real, $\omega_{3,4}$ are complex conjugates), and

$$
\begin{aligned}
A &= \frac{1}{(\omega_1 - \omega_2)((\Re(\omega_3)^2 + \Im(\omega_3)^2) - \omega_1(2\Re(\omega_3) - \omega_1))} \\
B &= -A\frac{\Re(\omega_3)^2 + \Im(\omega_3)^2 - \omega_1(2\Re(\omega_3) - \omega_1)}{\Re(\omega_3)^2 + \Im(\omega_3)^2 - \omega_2(2\Re(\omega_3) - \omega_2)} \\
C &= -(A + B) \\
D &= A(2\Re(\omega_3) - \omega_1) + B(2\Re(\omega_3) - \omega_2).
\end{aligned}
$$

where $\Re$ and $\Im$ denote the real and imaginary parts of complex numbers, respectively.

Surprisingly, our result is the same solution as presented by Besson [24], even though he modeled a different, but similar, physical problem. Besson however assumed some simplifications, different assumptions from ours, and solved the differential equation via other methods. Nonetheless his solution also contains three *logarithms*, one of them containing a second-order polynomial, and an *arctan*. Because of Besson's simplifying assumptions, however, his equation is limited to the case where $T - T_a = T + \frac{\eta_1}{\eta_0}$, which is a special case of our initial problem.

Similarly to actively cooled system, the passively cooled system will tend towards an equilibrium temperature T_e only if Equation 9 equates to zero. Given that an equilibrium temperature T_e exists, the convective heat transfer coefficient h_{pc} must be such that

$$h_{\mathrm{pc}} = \frac{\eta_1 T_e + \eta_0 + \epsilon\sigma S(T_a^4 - T_e^4)}{S(T_e - T_a)}, \qquad (13)$$

where all constants $\{T_e, T_a, e, S, \eta_1, \eta_0\} \in \mathbb{R}^+$. Consequently, this is only possible if $T_e > T_a$, as in the case of active cooling, and $\eta_1 T_e + \eta_0 > \epsilon\sigma S(T_a^4 - T_e^4)$.

The accurate solution for passively cooled objects as presented in Equation 10 is a function of the temperature: $t(T)$. For practical reasons, such as for DTMs, TMUs, and proportional-integral-derivative (PID) control techniques, an analytical formulation in the form of $T(t)$ is preferred. Inverting the exact solution is however, not a straightforward task, mainly because the *arctan* is hard to deal with as it keeps recurring. Numerical approaches will thus be preferred to compute this exact inverse solution. In Section 3.5 we will discuss approximations to the exact solution.

3.4 Experimental Validation of the Accurate Cooling Law Applied to a Microprocessor

To validate the passive cooling solution defined in Equation 10, we setup a set of CFD simulations in COMSOL where we analyze the transient thermal behavior of a slice of silica glass (SiO$_2$), as silica glass is closest to the thermal properties of a microprocessor. A 3D conjugate heat transfer scenario was created, with simulation settings as shown in Table 1. The exact same values, as listed in this table, were also used in our theoretical model. To approximate an isothermal object in COMSOL we have multiplied the thermal conductivity of the silica glass by 10^3. The silica glass has a surface area of $0.01\,\mathrm{m}^2$. For the heating process T_0 is set to 25°C and T_e is scaled between T_0 and 45°C. Similarly, for the cooling process T_0=45°C and T_e is scaled between T_0 and 25°C. The temperature values we chose correspond to what is typically encountered when using a mobile device. We used linear internal heat generation with the parameters as shown in Table 1. The convective heat transfer coefficient h_{ac} was set (Equation 13) such that with the given internal heat generation the predefined equilibrium temperature is attained. We look at two different levels of internal heat conversion, derived from ARM Cortex A15 quad-core processor power measurements on the Exynos 5210 Systems-on-Chip (SoC) [4]. The minimum internal heat conversion represents the A15 processor running a single applications at minimum processor frequency, whereas the

TABLE 1
Variables used for the COMSOL validation simulations. Specific values were calculated for the convective heat transfer coefficient (h_{ac}) and internal heat generation (ihg) such that a predefined equilibrium temperature is attained.

CONSTANTS		
symbol	value	dim.
σ	5.670×10^{-8}	W/(m^2·K^4)
ϵ	0.94	-
T_a	20	°C
D	2	mm
S	0.01	m^2
C	$S \times D \times 1548709$	J/K
VARIABLES		
symbol	VALUE	dim.
	ihg min	ihg max	
$heating : h_{\mathrm{ac}}$	-4.359	11.144	W/(m^2·K)
$cooling : h_{\mathrm{ac}}$	2.764	76.939	W/(m^2·K)
η_1	1.053	9.407	W/K $\times 10^{-3}$
η_2	0.098	1.318	W

maximum internal heat conversion represents the A15 processor running at maximum frequency while executing four applications in parallel.

Figure 1 shows the transient thermal behavior of the silica glass as described above. On the left the case for maximum internal heat generation is shown and on the right for minimum internal heat generation. Both the cooling and heating process are shown in the same graph. We have also generated data for various surface areas and equilibrium temperatures; since all graphs look similar we don't show all of them. Our theoretical model curves follow the experimental COMSOL curves well. The maximum temperature difference between our model and the COMSOL results is less than 0.5°C. Interestingly, the COMSOL transient data seems to have a slightly steeper slope than our theoretical model. This could be originating from the fact that the COMSOL object is not 100% isothermal. Despite the small temperature discrepancy between our analytical model and the COMSOL data we may deem our model an appropriate solution for passive cooling with internal heat generation.

3.5 Approximations of the Accurate Cooling Law

The accurate solution for the passive heat Equation 10 is of the form $f(T) = t$. Ideally, for practical motivations, we would like to know the inverse $f(t) = T$. For example, this may be convenient for the equation to be used in PID controller systems. Calculating the inverse of Equation 10 is, however, a challenging endeavor. Therefore, we will utilize effective approximations to obtain an invertible heat equation.

Finding a useful expression $f(t) = T$ requires isolating T in Equation 10. Mainly the presence of the *arctan* throws a monkey wrench in the mathematical derivation. Linearization or differential approximation will not provide any help as the derivative within the pertinent temperature range, i.e. between 25°C and 45°C, is far from being constant. Converting the *arctan* into a logarithm introduces imaginary numbers; yet, applying complex exponentiation rules will not get rid of the *arctan*. The *arctan* keeps recurring further on in the derivation. So we need to walk different paths to come to a solution for $f(t) = T$.
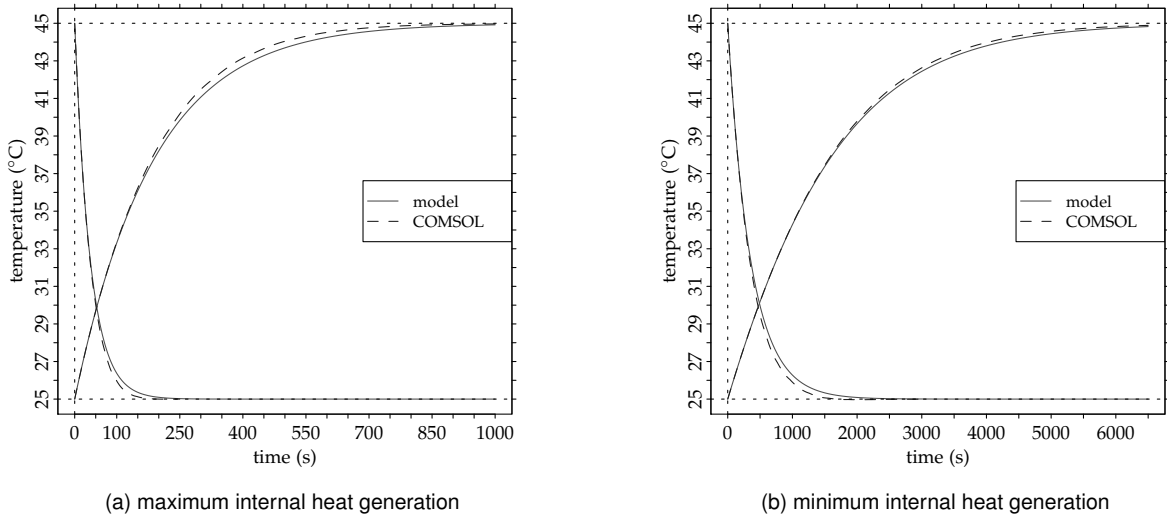
(a) maximum internal heat generation   (b) minimum internal heat generation

Fig. 1. Transient thermal behavior as per COMSOL and our analytical model.

TABLE 2
Overview of approximations to the accurate passive cooling law.

APPROXIMATION	$T(t)$
Coefficient	$T = \dfrac{\omega_1 \pm \omega_2 c_o e^{-\frac{\kappa_2}{A}t}}{1 \pm c_o e^{-\frac{\kappa_2}{A}t}}$
O'Sullivan 1st	$T = \left(T_0 - T_a + \frac{p}{n}\right) e^{-\frac{n}{C}t} - \frac{p}{n} + T_a$
O'Sullivan 2nd	$T = \dfrac{\omega_1 \pm \omega_2 c_o e^{-\frac{m}{A}t}}{1 \pm c_o e^{-\frac{m}{A}t}}$

Table 2 shows an overview of three different approximations that we will consider. The derivation and motivation behind each approximation, as well as the definition of all the variables, are expounded in Appendix C. In short, the *coefficient approximation* models the radiation within a specific temperature range with a quadratic polynomial. This reduces Equation 9 to a second-order problem. The *first* and *second O'Sullivan approximations* are based on a binomial expansion that mingles the coefficients of Equation 9 in a deterministic manner. The advantage is that the resulting equation is invertible when higher-order coefficients are dropped. Also, the accuracy of the approximation can be controlled by the degree of coefficients selected. As can be observed from Table 2 the coefficient approximation and the second-order O'Sullivan approximation are similar in shape. However, the definition of their respective variables have no common ground.

Let us analyze the accuracy of the approximations. We define the measure of accuracy as the root-mean-square error (RMSE) between the accurate cooling solution ϕ and an approximate solution ψ for n samples:

$$\text{RMSE} = \sqrt{\frac{\sum_{i=0}^{n}(\phi_i - \psi_i)^2}{n}}, \qquad (14)$$

where n is the number of samples over which RMSE is computed. We defined n=500 and equally spaced between $t \in \{0, t(0.99 \cdot T_e)\}$ (see Equation 10 for $f(T)$=t). The accurate cooling law and its approximations are generated with the same constants as the COMSOL simulation in the previous section in Table 1. We investigate the accuracy while changing surface area S, internal heat generation (ihg), equilibrium temperature T_e, for the cooling and warming process separately. We set T_0=25°C for the heating process and T_0=55°C for the cooling process. We variate the equilibrium temperature T_e between 25°C and 55°C. The convective heat transfer coefficient is computed accordingly to attain the respective equilibrium temperature based on Equation 13. The variables generated for the accurate cooling law are then used to compute the approximations.

Figure 2 shows the RMSE of the approximations for different surface areas, internal heat generation and equilibrium temperature settings. From all graphs the coefficient approximation is clearly performing best. Also, the second-order O'Sullivan approximation is considerably better than the first-order O'Sullivan approximation. However, for very small surface area the errors in all approximations are acceptable. Interestingly, the first-order O'Sullivan approximation does well for small surface areas, because the radiative part in the heat equation becomes negligible for smaller surface areas, and so the passive heat equations tends towards an exponential cooling law (see next section). Consequently the first-order O'Sullivan approximation, being an exponential function, is able to approximate the accurate cooling law well for very small surface areas: $S < 0.005$.

The errors for small internal heat generation seem to be systematically larger than the errors for the maximum internal heat generation case. The same observation can be made for the heating and cooling processes. The heating approximation seems to be more erroneous than the cooling process.

For variable equilibrium temperatures we see that for $|T_0 - T_e|$ the error increases for the heating process and decreases for the cooling process. In the derivation of the O'Sullivan approximations we have assumed that $T - T_a$ remains relatively small. This implies that the larger T departs from T_a the more imprecise the approximation becomes. For the cooling process T_0=55°C and the equilibrium temperature T_e was scaled between 25°C and 55°C.

(a) maximum internal heat generation

(b) minimum internal heat generation

(c) maximum internal heat generation
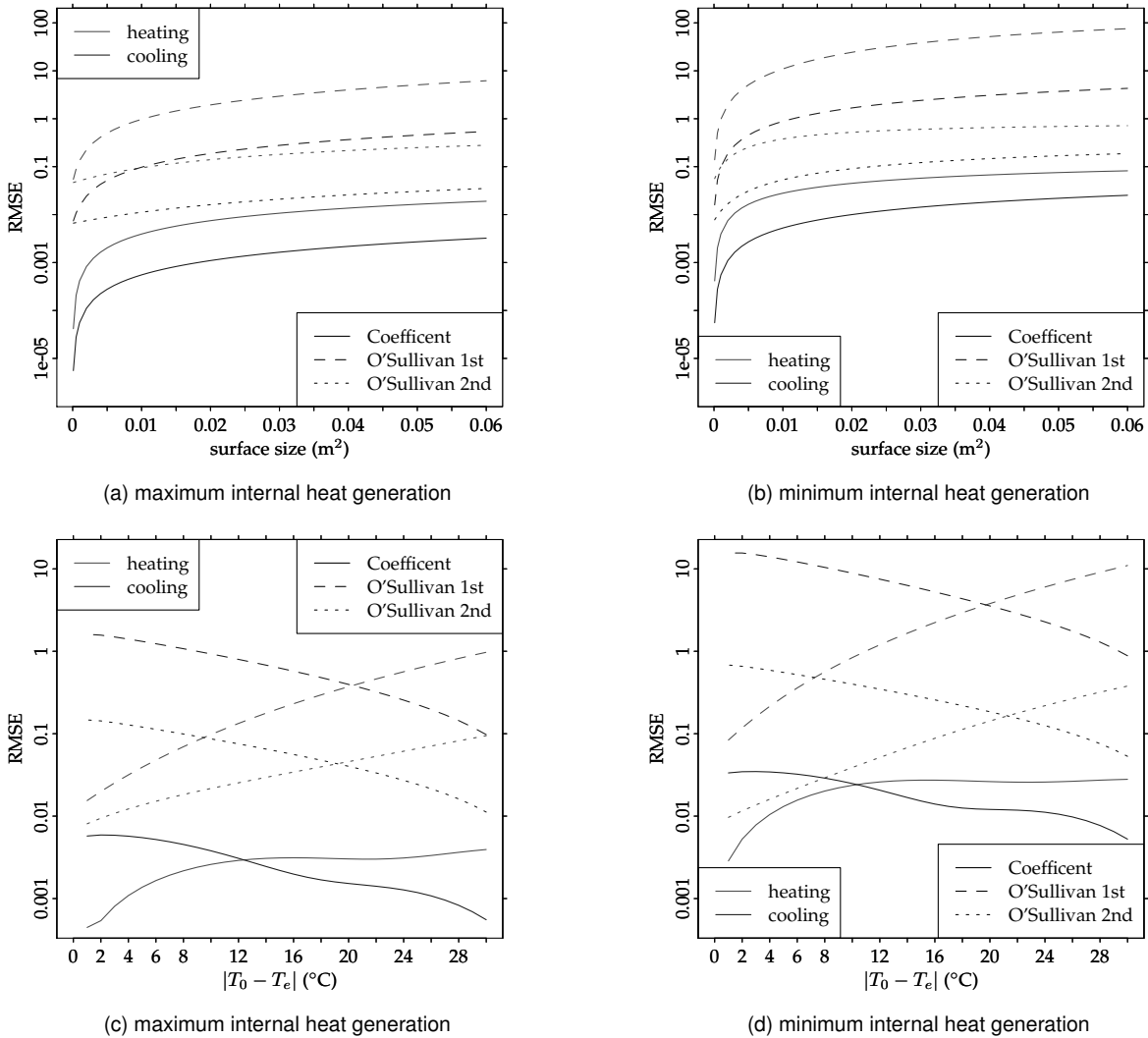
(d) minimum internal heat generation

Fig. 2. Root mean-square error RMSE between the accurate cooling law and the approximations. On top (a,b) the surface area S is variable, whereas the equilibrium temperature T_e is variable in the bottom graphs($S = 0.01\text{m}^2$) (c,d). The *Coefficient Approximation* seems to outperform the other approximations. The *Second-order O'Sullivan approximation* is performing acceptably as well for small values of $|T - T_a|$.

Similarly, for the heating process T_0 was set to 55°C and T_e was scaled between 25°C and 55°C. In both cases T_a was fixed to 20°C. Thus as the cooling process approaches T_a for increasing $|T_0 - T_e|$, $T - T_a$ becomes smaller, and hence also the error between the O'Sullivan approximations and the exact cooling law. The reverse observation is also valid for the heating process; RMSE becomes larger for larger values of $T - T_a$. The error properties in the case of the coefficient approximation is dependent on the fit of the second-order polynomial on the (quadratic) radiation function.

Overall, we do not advise to use the first-order O'Sullivan approximation, unless the surface area is really small. The second-order O'Sullivan approximation can be used but with caution. The equilibrium temperature should not depart too much from the ambient temperature T_a; $T - T_a$ <15°C seems acceptable. We recommend, however, the use of the coefficient approximation, even though the solution isn't much elegant when the large polynomial coefficients are introduced.

4 COMPARISON OF THE PASSIVE AND ACTIVE COOLING LAWS

Given the intrinsic complexity of the (inverse) function describing passive cooling compared to the rather straightforward exponential specification of other cooling modes, it is worth investigating in which cases dealing with it is necessary in practice. We ran a series of simulations to understand under what circumstances the passive and active cooling laws differ from each other. The main difference between the active and the passive cooling laws is the presence of the radiative heat transfer mode. Thus, if the radiative heat transfer is negligible compared to the convective heat transfer, the passive cooling law will approach an exponential cooling law. We explore when such situations occur based on concrete microprocessor use cases.

Let us recall that, for an isothermal body with internal heat generation, Equation 6 governs active cooling and Equation 10 governs passive cooling, where $H(T)$ is a function of the temperature T defining the internal heat generation of the body. We have shown [4] that $H(T)$ is well

TABLE 3
Variables used for the simulation of the active and passive cooling laws.

Constants		
symbol	value	dim.
σ	5.670×10^{-8}	$W/(m^2 K^4)$
ϵ	0.94	-
T_a	20	$°C$
D	2	mm
Variables		
symbol	value	dim.
S	$[0, 6] \times 10^{-3}$	m^2
C	$S \times D \times 1708800$	J/K
T	$[25, 85]$	$°C$
h	(see Equation 7/13)	$W/(m^2 K)$
$\alpha_{\min,\max}$	$\{0.396, 4.030\}$	W
$\beta_{\min,\max}$	$\{29.015, 32.010\}$	-
$\gamma_{\min,\max}$	$\{82.738, 149.797\}$	-

described by an exponential equation. Even more, within the temperature range $25°C < T < 55°C$, the exponential can be approximated well with a linear or quadratic polynomial. Yet, for the more extended temperature range $25°C < T < 85°C$, an exponential function is advised.

We compare the active and passive cooling of a microprocessor in the context of an embedded system, i.e., a low-power processor subject to internal heating generation and cooling. In order to do so, we assume a simplified microprocessor model: an isothermal volume, with the physical properties of silica glass, and cooled via convection and radiation. Table 3 shows the values used in our simulations. The table lists the fixed variables: σ, ϵ, T_a and D. We chose the emissivity of PVC for ϵ and fixed T_a to be a representative room temperature. The height of our microprocessor D is characteristic for a modern SoC. The variables that may vary during the analysis are also listed. We study the impact of the surface area S over which the device cools via convection and radiation. The minimum size was set to a square with a side of $1\,cm$. This is representative for a small SoC; for example, the Samsung Exynos 5 SoC has a side length of $1.6\,cm$. The maximum surface area was set to $0.1\,m^2$, which is a representative area for a large tablet. We analyze the behavior of the system within the temperature range $T \in [25, 85]°C$. Throughout the analysis, we define the internal heat generation $H(T)$ to be an exponential function $(\alpha + e^{(T-\gamma)/\beta})$; the coefficients are shown in Table 3 as pairs. The left values are for minimal internal heat generation, the right values for maximum internal heat generation. The values for α, β and γ were derived from power and temperature measurements on a SoC sporting a CORTEX A15 [4]. We measured the system's power consumption when the A15 is running at full capacity, i.e. at $1.6\,GHz$, and when the A15 is running in low-power mode, i.e. at $800\,MHz$. The heat capacity of the body C is the product of its volume $S \times D$ and its specific heat and density $(\approx 2.4 \times 10^6 \cdot 0.712)$.

4.1 Relative Heat Transfers

First, we look at the ratio of the convective heat transfer coefficients of the passive and active cooling cases. The temperature T_0 at $t=0$ is set to $25°C$. Then we compute the respective convective heat transfer coefficients as per Equation 13 and Equation 7 based on a series of equilibrium temperatures T_e. The ratio of the convective heat transfer coefficients r_{cr} is given by

$$r_{cr} = \frac{h_{pc}}{h_{ac}} = \frac{\epsilon \sigma S(T_a^4 - T_e^4) + H(T_e)}{H(T_e)}.$$

r_{cr} shows how much the active and passive cooling laws will resemble. If $r_{cr} = 1$, there is no difference between the two cooling cases. The more r_{cr} tends to zero, the more the two cooling laws will deviate in behavior.

Figure 3 shows the ratio of the convective heat transfer coefficient of the passive and active cooling cases. Given that r_{cr} stays well above 0.95, it is observed that, for a small object, similar to SoCs (left most vertical dashed line), the difference between active and passive cooling will be very small for all equilibrium temperatures ranging between $20°C$ to $85°C$. For a moderate surface area, e.g., the size of an average smartphone (middle vertical dashed line), the radiative cooling starts to become more prominent already for temperatures close to the ambient temperature T_a. For equilibrium temperatures more than about $5°C$ above T_a, signs of deviating behavior will become clearly visible. Large surface areas and equilibrium temperatures close to T_a will yield a r_{cr} that is smaller than 0.95. This implies that the radiative cooling for large surfaces has to be taken into account. As a general rule of thumb, we can say that the larger the equilibrium temperature and the cooling surface, the more behavioral differences between passive and active coolings will occur. So how large are the differences temperature-wise in particular?

4.2 Temperature Differences

When looking at the temperature differences between the passive and active cooling laws at specific points in time, we must differentiate between the cooling and heating processes. Convective heat transfer is proportional to the difference of the body temperature and the ambient temperature, and is therefore *independent* on the absolute temperature of the body and environment. This results in a symmetry between the heating and the cooling processes for convective heat transfer. The radiative heat transfer, on the other hand, is *dependent* on the absolute values of the body and the environment. This is illustrated as follows for the convective and radiative heat transfers respectively:

$$
\begin{aligned}
|hS(T - (T - x))| &= |hS(T - (T + x))| \\
|\epsilon \sigma S(T^4 - (T - x)^4)| &\neq |\epsilon \sigma S(T^4 - (T + x)^4)| \quad (15)
\end{aligned}
$$

As a consequence, due to the last inequality, the radiative heat transfer process will not be symmetric for the cooling and heating processes. Moreover, when radiative heat transfer is combined with convective heat transfer, the symmetry property of the heating and cooling processes will not hold either.

Let us define the temperature lag ΔT between an actively and passively cooled identical body, measured at the moment when the passively cooled body reaches a reference temperature T_{pc}. The reference temperature T_{pc} is henceforth defined as $T_{pc} = 0.85(T_e - T_0) + T_0$, i.e., when the

(a) maximum internal heat generation   (b) minimum internal heat generation
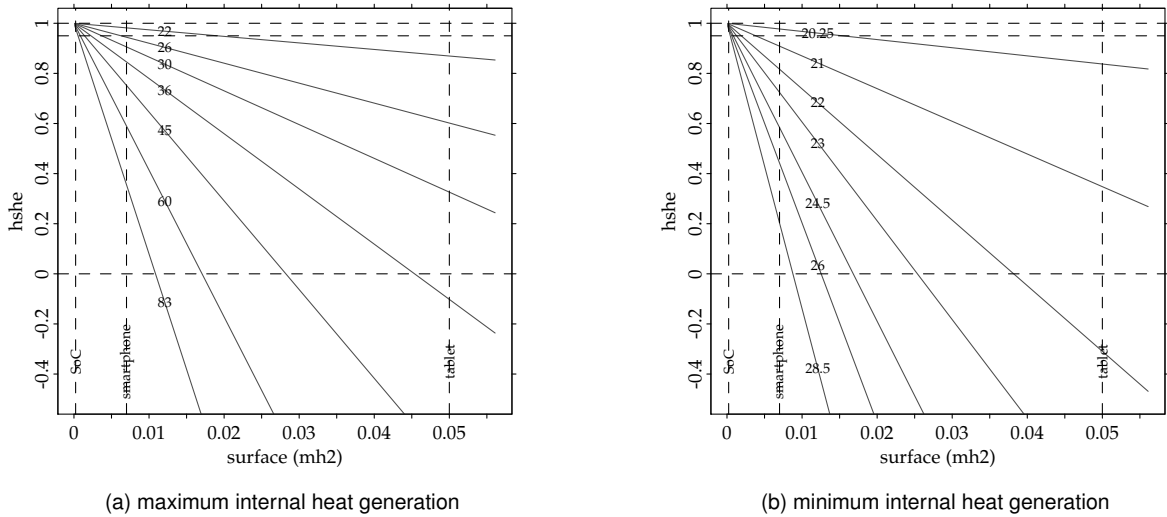
Fig. 3. Ratio between the convective heat transfer coefficients of active and passive coolings at a given equilibrium temperatures T_e (see curve labels in °C). In Figure (a) the internal heat generation is set to a maximum, while in (b) it is set to a minimum. The vertical dashed lines represent typical surfaces of a SoC ($\approx 2.5\,\mathrm{cm}^2$), a smartphone ($\approx 70\,\mathrm{cm}^2$) and a tablet ($\approx 5\,\mathrm{dm}^2$). A horizontal reference line is drawn at $r_{\mathrm{cr}} = 0.95$.

body temperature has reached 85% of its equilibrium temperature, starting from T_0. It is also assumed that both the passively and actively cooled bodies have the same internal heat generation process and initial condition T_0 at $t = 0$. Figure 4 shows the relative temperature lag $\Delta\tau$, which is defined as the absolute temperature lag ΔT divided by the temperature difference at $t = 0$ and at equilibrium $|T_e - T_0|$:

$$\Delta\tau = \frac{\Delta T}{|T_e - T_0|} = \frac{T_{\mathrm{pc}} - T_{\mathrm{ac}}}{|T_e - T_0|}. \tag{16}$$

The relative temperature lag $\Delta\tau$ is depicted in Figure 4 for both a large and a small internal heat generation, as defined before, and for the heating and cooling processes separately.

A reference line is drawn for $\Delta\tau = 5\%$. Data points on the right of the dashed blue line show configurations with one or more negative convective heat transfer coefficients. This implies that in these cases additional heat needs to be added to attain the given equilibrium temperature. These data points are however, not of concern in our work.

For the case of large internal heat generation, the relative temperature lag $\Delta\tau$ for small surfaces stays below 0.5%, meaning that the presence of radiative heating will be quasi unnoticeable here. $\Delta\tau$ stays around 5% in the case of small internal heat generation, which may be difficult to spot. Contemporary on-die processor temperature sensors report frequently temperatures in steps of 1°C. Given this quantization noise, a relative temperature lag of 5% could be hard to identify when $|T_e - T_0| > 20°$C. So for small processor temperature variations, it is again unlikely that a contemporary processor temperature sensor is able to distinguish between active and passive cooling. For a smartphone-size cooling surface, the relative temperature lag varies significantly depending on the situation. For a large internal heat generation and heating, there is less than 5% difference between passive and active cooling. For the other cases, however, the discrepancy between the passive and active cooling can run up from nil to as high as 10%, depending on the equilibrium temperature. $\Delta\tau = 10\%$ is

already noticeable at $|T_e - T_0| > 10°$C in the presence of 1°C quantization noise. The data for the tablet-sized cooling surfaces is mostly not of our concern as the convective heat transfer coefficients for passive and active cooling are negative. This means that heat needs to be added to the system to attain the given equilibrium temperature.

Generally speaking, we notice that the relative temperature lag $\Delta\tau$ for heating cases is smaller than for the cooling cases. This can be explained via the inequality of Equation 15. The radiative heat transfer coefficient will have greater weight when the body's temperature is larger than the equilibrium temperature than when the temperature is below the equilibrium, hence inflating the discrepancy between active and passive cooling. Also, the amount of internal heat generation affects the relative temperature lag. It appears that the larger the internal heat generation, the smaller $\Delta\tau$ becomes. Indeed, given the differential representation of the cooling law in Equation 8, we see that the internal heat generation can outweigh the radiative and convective coolings the larger it becomes. Thus the larger the internal heat generation, the less sensitive the body becomes to changes in the radiative or convective cooling, and the more active and passive cooling will resemble.

5 CONCLUSION

We have developed an accurate cooling law for passively cooled objects subject to radiation, (natural) convection, and internal heat generation. The passive cooling law is analytically more complex than the commonly accepted exponential cooling law (which is technically sound for forcibly cooled objects). Unfortunately, the accurate solution for the passively cooled object is a function of temperature: $t(T)$. Numerical approaches can be used for the computation of the exact inverse: $T(t)$. The validation of the passive cooling law's accurate solution via CFD simulations demonstrated the cooling law's adequacy.

Via analytical simulations, we showed that the difference between active and passive cooling depends on three

(a) cooling – max internal heat generation

(b) cooling – min internal heat generation

(c) cooling – max internal heat generation
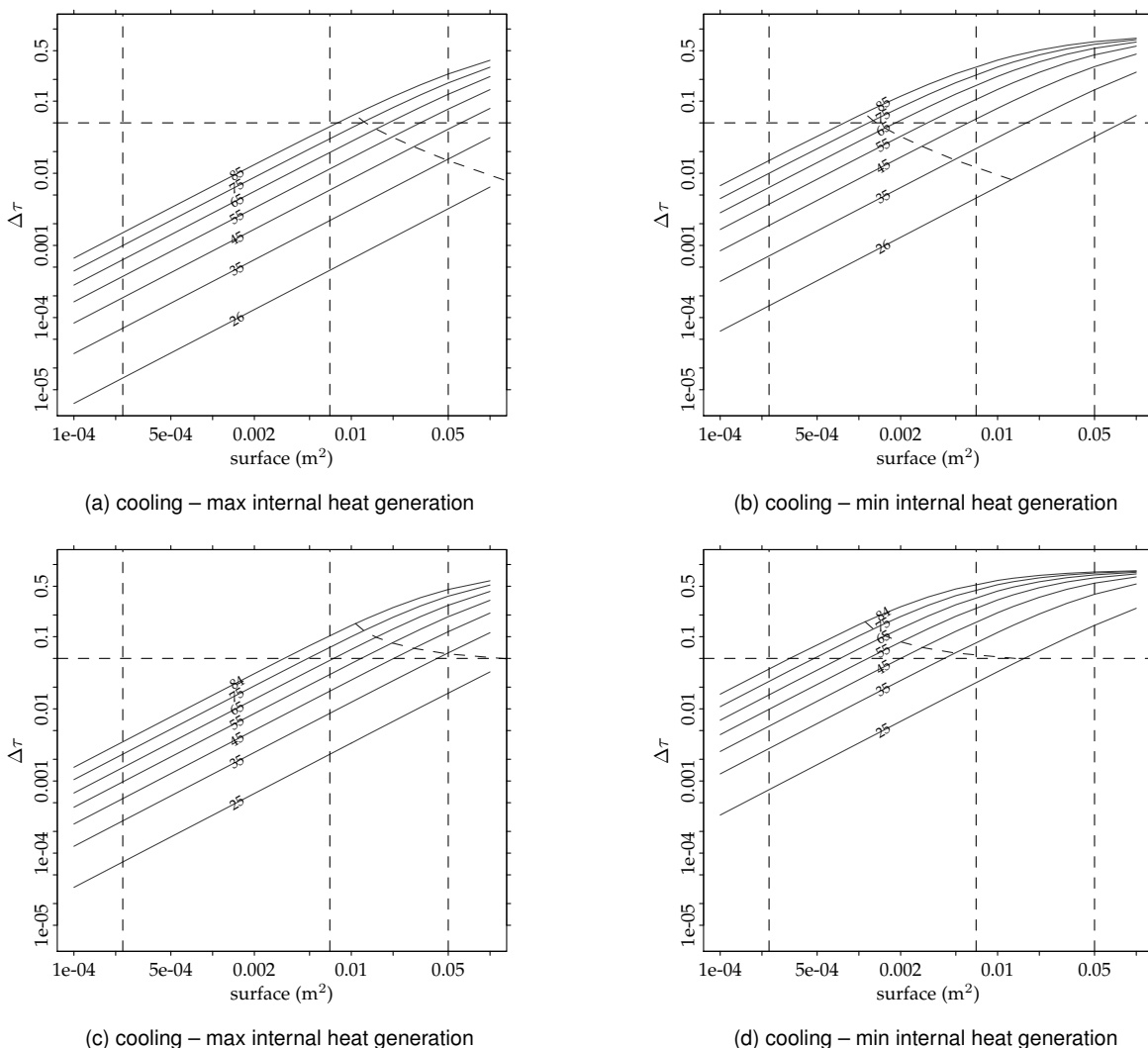
(d) cooling – min internal heat generation

Fig. 4. Relative time lag $\Delta\tau$ (Equation 16) for the internal heat generation set to the maximum (a,c), and set to the minimum (b,d). The curves are generated for different equilibrium temperatures (see curve labels in $^\circ$C). On the top row, the heating process is depicted (a,b), with the cooling process on the bottom row (c,d). The three vertical dashed lines represent typical surfaces for a SoC ($\approx 2.5\,cm^2$), a smartphone ($\approx 70\,cm^2$) and a tablet ($\approx 5\,dm^2$). Data points on the right of the blue dashed lines have negative convective heat transfer coefficients.

factors: 1) the surface area of the object, 2) the internal heat generation, and 3) the equilibrium temperature. For large objects, we showed that the difference between active and passive cooling can be significant. For medium-sized ones, depending on the magnitude of the internal heat generation and equilibrium temperature, the discrepancy between active and passive cooling could tentatively go unnoticed. For small surfaces, e.g., SoCs, an exponential cooling law is shown to be an appropriate approximation. We also highlighted that the quantization noise of temperature sensors may conceal temporal information between active and passive cooling. As the cooling law for passively cooled devices is quite elaborate to work with and the possible uses of a scientifically sound cooling law by TMUs are limited by the lack of accurate temperature sensors, we can state that, for systems minimizing overhead, assuming an exponential cooling law will likely not induce large perceptual deviations from reality.

In this work we considered the cooling of an isothermal object. In practical situations this assumption doesn't always hold. To obtain a more realistic model we need to consider internal conduction and hence also thermal hotspots. Their impact on our heat model of these considerations is part of our future work. Moreover, in embedded systems, a microprocessor is usually mounted on a PCB and covered by other objects, such as an LCD display, radio interface and others. The presence of these objects also interacts with the passive cooling of the microprocessor. Most likely numerical methods will have to be deployed to gain more understanding under such conditions.

APPENDIX A
APPLICABILITY OF THE PASSIVE HEAT EQUATION

Previously we assumed that the internal heat generation $H(T)$ was a linear function, i.e., polynomial of the first-order with coefficients elements of $\mathbb{R}^+$. Given that the radiation absorbed or emitted by a body is described by a 4th-order polynomial, we discuss the implications of an arbitrary $H(T)$ up to the 3th-order. We will show via logical
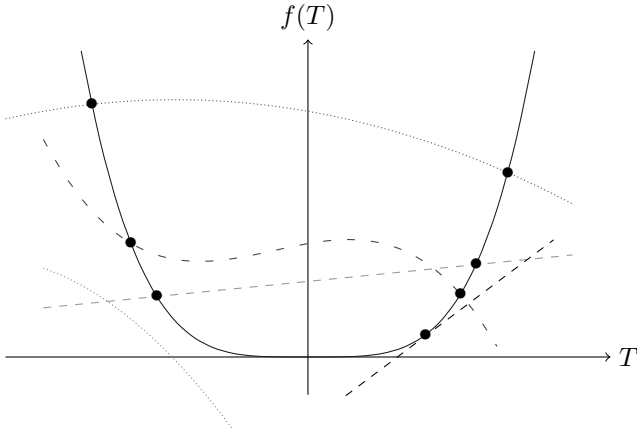
$f(T)$

Fig. 5. Visualization of Equation 18 for several variations of the right-hand side polynomial ($K(T)$). Polynomials: 1st order (dashed), 2nd order (dotted), 3rd order (loosely dashed), and δT^4 (solid). The black bullets represents the intersections of each polynomial with δT^4.

reasoning that the analytic solution in the paper holds for $H(T)$ up to the 3th order under certain conditions.

Let us define a body that is radiating energy at a rate $-\delta$, and subject to other heat transfer mechanisms described by a polynomial $K(T)$, e.g., internal heat generation. Let $K(T)$ be a polynomial of an order not larger than three. Then the thermal energy storage rate into the body is equal to:

$$C\frac{dT}{dt} = -\delta T^4 + K(T) = -\delta T^4 + (\kappa_3 T^3 + \kappa_2 T^2 + \kappa_1 T + \kappa_0),$$
(17)

where we define $\delta \in \mathbb{R}_0^+$, $\kappa_{0,1,2,3} \in \mathbb{R}$, and C is the thermal capacity of the system. δ must be positive as $-\delta T^4$ represents the heat emitted by the body via radiation. $\kappa_{0,1,2,3}$ are the constants of a polynomial describing the function $K(T)$. To solve the differential in Equation 17 the roots need to be found. In particular, we have solved the differential equation for a 4th-order polynomial assuming two real and two complex conjugate roots. To find the roots of Equation 17 we evaluate it at the equilibrium temperature $T = T_e$, then $dT/dt = 0$:

$$\delta T^4 = \kappa_3 T^3 + \kappa_2 T^2 + \kappa_1 T + \kappa_0.$$
(18)

This equality is visualized in Figure 5. There the solid blue curve represents the contribution on the left-hand side and the other dashed lines are possible examples of the polynomial in the right-hand side. It can be seen that it is easy to construct polynomials that have one or two intersections with δT^4. Also curves can be constructed that intersect the δT^4 only in one point (for example the dashed black line in Figure 5); such points are counted as two roots. The dashed gray line is an example of a polynomial without any intersection with δT^4. Only those polynomials with one or two intersections with δT^4 have physical meaning in the context discussed in this paper. One or two intersections with δT^4 produce two real roots and two complex conjugate roots. No intersections with δT^4 would imply that there exists no equilibrium temperature, i.e., the system is not thermally stable.

APPENDIX B
SOLVING THE PASSIVE HEAT EQUATION

The differential formulation of a passively cooled object with linear internal heat generation can be described as follows, as per Equation 9:

$$\frac{dT}{dt} = \frac{1}{C}(-\epsilon\sigma S T^4 + (\eta_1 - hS)T + (\eta_0 + S(hT_a + \epsilon\sigma T_a^4))).$$

The right-hand side is a fourth-order polynomial and the equality can be rephrased as:

$$\frac{dT}{dt} = -\kappa_4 T^4 + \kappa_3 T^3 + \kappa_2 T^2 + \kappa_1 T + \kappa_0,$$
(19)

where the constants $\kappa_4 \in \mathbb{R}_0^+$ and $\kappa_{\{0,1,2,3\}} \in \mathbb{R}^+$. Rearranging this equation yields

$$\int \frac{1}{T^4 - \frac{\kappa_3}{\kappa_4}T^3 - \frac{\kappa_2}{\kappa_4}T^2 - \frac{\kappa_1}{\kappa_4}T - \frac{\kappa_0}{\kappa_4}}dT = -\kappa_4 \int dt$$
(20)

The integration of the fraction on the left-hand side can be achieved via partial fractions decomposition:

$$\int \frac{1}{(T-\omega_1)(T-\omega_2)(T-\omega_3)(T-\omega_4)}dT$$
(21)

The roots ω_* of the 4th order polynomial in the denominator can be obtained via Ferrari's theorem, and other approximate methods such as Netwon's and the secant. Given that there exist a maximum of one or two real unique values for T that satisfy

$$\kappa_4 T^4 = \sum_{i=0}^{3} \kappa_i T^i,$$

we can state that two roots are real, say $\omega_{\{1,2\}}$; the other two roots are complex conjugates[1]. This means that $\Re(\omega_3) = \Re(\omega_4)$ and $\Im(\omega_3) = -\Im(\omega_4)$, which simplifies a few things. As the initial differential equation is real, we are looking for a real solution too; thus the imaginary part must equate to zero. This is however automatically taken care of as the product of the two complex roots yield a real sum:

$$\frac{1}{(T-\omega_3)(T-\omega_4)} = \frac{1}{(T-\Re(\omega_3))^2 + \Im(\omega_3)^2}.$$

Whence, Equation 21 becomes

$$\int \frac{A}{(T-\omega_1)} + \frac{B}{(T-\omega_2)} + \frac{CT+D}{(T-\Re(\omega_3))^2 + \Im(\omega_3)^2} \, dT.$$ (22)

Henceforth we define $\alpha = \Re(\omega_3)$ and $\beta = \Im(\omega_3)$. The values for A, B, and D are found by equating Equation 21 and Equation 22, which can be expressed as a system of equations:

$$\begin{cases} 0 &= A + B + C \\ 0 &= D - \omega_1(B+C) - \omega_2(A+C) - 2\alpha(A+B) \\ 0 &= \alpha^2(A+B) + \beta^2(A+B) + 2\alpha(\omega_2 A + \omega_1 B) \\ &\quad -(\omega_1 + \omega_2)D + \omega_1\omega_2 C \\ 1 &= -\alpha^2(\omega_2 A + \omega_1 B) - \beta^2(\omega_2 A + \omega_1 B) + \omega_1\omega_2 D \end{cases}$$

---

1. Appendix A shows that for our applications this is the case.

and can be solved via Gaussian elimination. So we obtain the expressions for A, B, C and D:

$$A = \frac{1}{(\omega_1 - \omega_2)((\alpha^2 + \beta^2) - \omega_1(2\alpha - \omega_1))} \tag{23a}$$

$$B = -A\frac{\alpha^2 + \beta^2 - \omega_1(2\alpha - \omega_1)}{\alpha^2 + \beta^2 - \omega_2(2\alpha - \omega_2)} \tag{23b}$$

$$C = -(A + B) \tag{23c}$$

$$D = A(2\alpha - \omega_1) + B(2\alpha - \omega_2) \tag{23d}$$

Continuing with Equation 22, this yields:

$$A \ln|T - \omega_1| + B \ln|T - \omega_2| + \int \frac{CT + D}{(T - \alpha)^2 + \beta^2} dT + c_0,$$

where c_o is an integration constant. The last term on the right-hand side may be integrated via substitution, where $u = (T - \alpha)^2$, yielding $du = 2(T - \alpha)dT$, and also $v = \frac{T - \alpha}{\beta}$, giving $dv = \frac{1}{\beta}dT$:

$$\int \frac{CT + D}{(T - \alpha)^2 + \beta^2} dT$$
$$= \int \frac{C(T - \alpha)}{(T - \alpha)^2 + \beta^2} dT + \int \frac{\alpha C + D}{(T - \alpha)^2 + \beta^2} dT$$
$$= \frac{C}{2} \ln|(T - \alpha)^2 + \beta^2| + \frac{\alpha C + D}{\beta} \arctan\left(\frac{T - \alpha}{\beta}\right) + c_1.$$

where c_1 is an integration constant. Then the solution to Equation 22 is as follows

$$A \ln|T - \omega_1| + B \ln|T - \omega_2| + \frac{C}{2} \ln|(T - \alpha)^2 + \beta^2|$$
$$+ \frac{\alpha C + D}{\beta} \arctan\left(\frac{T - \alpha}{\beta}\right) + c_1, \tag{24}$$

where A, B, C and D are given in Equations 23, and ω_* are the real roots of the polynomial in the denominator on the left-hand side, $\alpha = \Re(\omega_3)$, $\beta = \Im(\omega_3)$, and c_1 is a (new) integration constant satisfying the initial conditions.

Now we can complete Equation 20:

$$t = -\frac{1}{\kappa_4}\left(A \ln|T - \omega_1| + \frac{C}{2} \ln|(T - \alpha)^2 + \beta^2| + c_o\right.$$
$$\left. + B \ln|T - \omega_2| + \frac{\alpha C + D}{\beta} \arctan\left(\frac{T - \alpha}{\beta}\right)\right).$$

APPENDIX C
DERIVATIONS OF APPROXIMATIONS FOR $f(T) = t$

The exact passive cooling law as presented is of the form $f(T) = t$. For practical reasons we desire a formulation of the form $f(t) = T$. Unfortunately inverting the exact passive heat equation is challenging. We develop three approximations to the exact passive cooling law which are more easily invertible.

C.1 Quadratic Approximation

Stefan-Boltzmann's law of radiation states that the energy emitted by radiation is proportional to T^4 (Equation 2). Because of this term the polynomial of Equation 9 is of the fourth-order. More specifically, it are the two imaginary roots of the fourth order polynomial that introduce the *arctan* in Equation 10. If we were to approximate T^4 with

a second-order polynomial and assert real roots, then we could get rid of the dependency of the *arctan*, and isolating T would be more straightforward. The quadratic approximation

$$\begin{aligned} T^4 &= q_0 + q_1 T + q_2 T^2 \\ &= 29700057265 - 251483462\,T + 598262\,T^2 \end{aligned} \tag{25}$$

introduces an error between -0.041% and 0.072% for $20°C < T < 65°C$, which is very acceptable. Then the quadratic approximation to Equation 19 would be equal to solving

$$\frac{dT}{dt} = \kappa_2 T^2 + \kappa_1 T + \kappa_0. \tag{26}$$

The solution to this equation, assuming two real roots ($\omega = (-\kappa_1 \pm \sqrt{\kappa_1^2 - 4\kappa_2\kappa_0}/(2\kappa_2))$) and that $\kappa_2 < 0$:

$$t = -\frac{1}{\kappa_2}\left(A \ln|T - \omega_1| + B \ln|T - \omega_2| + c_o\right), \tag{27}$$

where $A = 1/(\omega_2 - \omega_1)$ and $B = -A$. Now we can isolate T as follows:

$$t + \frac{c_o}{\kappa_2} = -\frac{A}{\kappa_2}\left(\ln|T - \omega_1| - \ln|T - \omega_2|\right)$$
$$-\frac{\kappa_2 t + c_o}{A} = \ln\left(\frac{|T - \omega_1|}{|T - \omega_2|}\right)$$
$$c_o e^{-\frac{\kappa_2}{A}t} = \frac{|T - \omega_1|}{|T - \omega_2|}.$$

Let's define ω_1 and ω_2 such that $\omega_1 < \omega_2$. As we are operating in the temperature range $0°C < T < 100°C$ and given the shape of the quadratic approximation, T will always be larger than ω_1. Hence we can assume that $T - \omega_1 > 0$. The absolute value of $T - \omega_2$ forces us to distinguish two cases, i.e. where $T > \omega_2$ and the case for $T < \omega_2$. Bear in mind that ω_2 is also the equilibrium temperature T_e of the system. This corresponds either to the heating or the cooling process, respectively. For $T > \omega_2$ we have

$$T - \omega_1 = (T - \omega_2)c_o e^{-\frac{\kappa_2}{A}t}$$
$$T = \frac{\omega_1 - \omega_2 c_o e^{-\frac{\kappa_2}{A}t}}{1 - c_o e^{-\frac{\kappa_2}{A}t}}$$

and accordingly for $T < \omega_2$, or the heating process, we get:

$$T = \frac{\omega_1 + \omega_2 c_o e^{-\frac{\kappa_2}{A}t}}{1 + c_o e^{-\frac{\kappa_2}{A}t}}, \tag{28}$$

where c_o is an integration constant to meet the initial condition $f(0) = T_0$, and given by

$$c_o = \frac{|T_0 - \omega_1|}{|T_0 - \omega_2|}.$$

The roots ω_* are are easily found as follows:

$$\omega_1 = \frac{-\kappa_1 + \sqrt{\kappa_1^2 - 4\kappa_2\kappa_0}}{2\kappa_2} \quad \text{and} \quad \omega_2 = \frac{-\kappa_1 - \sqrt{\kappa_1^2 - 4\kappa_2\kappa_0}}{2\kappa_2}.$$

The equilibrium temperature T_e is defined by the positive root ω_2.

In the above derivation, we have fixed the coefficients q_* in Equation 25. These values were chosen to fit best in a certain temperature range. To be more universally applicable, however, the coefficients could be generated dynamically such that they are optimally tailored to the temperature range of concern.

C.2 First Order O'Sullivan Approximation

O'Sullivan [25] presented an approximation for a cooling law including convection and radiation, but without the presence of internal heat generation. We extend his approximation with internal heat generation. We will use an alternative formulation of the internal heat generation such that we can more easily apply our variable substitution later on: $H(T) = \eta_1 T + \eta_0 = \eta_1(T - T_a) + \eta_1 T_a + \eta_0$. The initial definition of the passive heat Equation 9 then becomes:

$$-C\frac{dT}{dt} = \epsilon\sigma S(T^4 - T_a^4) + (hS - \eta_1)(T - T_a) - (\eta_1 T_a + \eta_0).$$

Let's introduce the variable $\theta = T - T_a$:

$$-C\frac{d\theta}{dt} = \epsilon\sigma S((\theta + T_a)^4 - T_a^4) + (hS - \eta_1)\theta - (\eta_1 T_a + \eta_0).$$

Now, we can apply binomial expansion to $(\theta - T_a)^4$, whence:

$$\begin{aligned} -C\frac{d\theta}{dt} &= \epsilon\sigma S((\theta^4 + 4T_a\theta^3 + 6T_a^2\theta^2 + 4T_a^3\theta \\ &\quad + T_a^4) - T_a^4) + (hS - \eta_1)\theta - (\eta_1 T_a + \eta_0) \\ &= k\theta^4 + l\theta^3 + m\theta^2 + n\theta + p, \end{aligned} \quad (29)$$

where the coefficients for surfaces around $1\,\mathrm{dm}^2$ are as follows:

$$\begin{aligned} k &= \epsilon\sigma S \quad (\sim 10^{-10}) \\ l &= 4\epsilon\sigma S T_a \quad (\sim 10^{-7}) \\ m &= 6\epsilon\sigma S T_a^2 \quad (\sim 10^{-5}) \\ n &= (hS - \eta_1 + 4\epsilon\sigma S T_a^3) \quad (\sim 0.01) \\ p &= -(\eta_1 T_a + \eta_0) \quad (\sim 1). \end{aligned}$$

Now, if $(T - T_a)$ is not too large the series on the right-hand side of Equation 29 converges reasonably fast [25]. Depending on the accuracy desired, the higher-order coefficients may be dropped. Let's see how well a first-order and a second-order approximation behaves. As expected, the first-order approximation yields also an exponential law:

$$-C\frac{d\theta}{dt} = n\theta + p \quad \Rightarrow \quad \theta = c_o e^{-\frac{n}{C}t} - \frac{p}{n},$$

where c_o is an integration constant such that $\theta(t = 0) = T_0 - T_a$:

$$c_o = \theta_0 + \frac{p}{n} = (T_0 - T_a) + \frac{p}{n}.$$

And so the first-order O'Sullivan solution is:

$$T = \left(T_0 - T_a + \frac{p}{n}\right)e^{-\frac{n}{C}t} - \frac{p}{n} + T_a. \quad (30)$$

C.3 Second-Order O'Sullivan Approximation

The second-order O'Sullivan approximation is a bit more complex compared to the first-order O'Sullivan approximation. Moreover, the derivation looks also significantly different from the original derivation of O'Sullivan [25], given the presence of the constant term p in Equation 29. The second-order O'Sullivan approximation is similar to the coefficient approximation in the sense that solving

$$-C\frac{d\theta}{dt} = m\theta^2 + n\theta + p \quad (31)$$

is similar to solving Equation 26. Thus the solution for the second-order O'Sullivan approximation will be the same as for the quadratic approximation, except for the constants definition. We can thus state that the second-order O'Sullivan approximation is given by:

$$T = \frac{\omega_1 \pm \omega_2 c_o e^{-\frac{m}{AC}t}}{1 \pm c_o e^{-\frac{m}{AC}t}} + T_a, \quad (32)$$

where "$\pm$" becomes "$+$" for $T_e > T_0$, and "$-$" for $T_e < T_0$. ω_* is given by:

$$\omega_1 = \frac{-\sqrt{n^2 - 4pm} - n}{2m} \quad \text{and} \quad \omega_2 = \frac{\sqrt{n^2 - 4pm} - n}{2m}.$$

The constant A and c_o, such that $\theta(0) = \theta_0$, are defined as:

$$A = -\frac{1}{\omega_2 - \omega_1} \quad \text{and} \quad c_o = \frac{|\theta_0 - \omega_1|}{|\theta_0 - \omega_2|},$$

where $\theta_0 = T_0 - T_a$. The equilibrium temperature T_e is defined by $\omega_2 + T_a$.

ACKNOWLEDGMENTS

REFERENCES

[1] J. Kong, S. W. Chung, and K. Skadron, "Recent thermal management techniques for microprocessors," *ACM Comput. Surv.*, vol. 44, no. 3, pp. 13:1–13:42, Jun. 2012.

[2] R. Viswanath, V. Wakharkar, A. Watwe, and V. Lebonheur, "Thermal performance challenges from silicon to systems," *Intel Technology Journal*, no. Q3, pp. 1–16, Aug. 2000.

[3] V. Hanumaiah and S. Vrudhula, "Reliability-aware thermal management for hard real-time applications on multi-core processors," in *Design, Automation Test in Europe Conference Exhibition (DATE), 2011*, March 2011, pp. 1–6.

[4] K. De Vogeleer, G. Memmi, P. Jouvelot, and F. Coelho, "Modeling the temperature bias of power consumption for nanometer-scale cpus in application processors," in *International Conference on Embedded Computer Systems: Architectures, Modeling, and Simulation (SAMOS XIV)*, jul. 2014.

[5] F. Zanini, D. Atienza, C. N. Jones, L. Benini, and G. De Micheli, "Online thermal control methods for multiprocessor systems," *ACM Trans. Des. Autom. Electron. Syst.*, vol. 18, no. 1, pp. 6:1–6:26, Jan. 2013.

[6] M. Gockenbach and K. Schmidtke, "Newton's law of heating and the heat equation," *Involve Mathematical Journal*, vol. 2, no. 4, pp. 439–450, Oct. 2009.

[7] W. Huang, S. Ghosh, S. Velusamy, K. Sankaranarayanan, K. Skadron, and M. Stan, "Hotspot: a compact thermal modeling methodology for early-stage VLSI design," *Very Large Scale Integration (VLSI) Systems, IEEE Transactions on*, vol. 14, no. 5, pp. 501–513, May 2006.

[8] S. Sarangi, G. Ananthanarayanan, and M. Balakrishnan, "Lightsim: A leakage aware ultrafast temperature simulator," in *Design Automation Conference (ASP-DAC), 2014 19th Asia and South Pacific*, Jan 2014, pp. 855–860.

[9] Y. Han, I. Koren, and C. M. Krishna, "TILTS: A fast architectural-level transient thermal simulation method," *J. Low Power Electronics*, vol. 3, no. 1, pp. 13–21, 2007.

[10] Y. Yang, Z. Gu, C. Zhu, R. Dick, and L. Shang, "ISAC: Integrated space-and-time-adaptive chip-package thermal analysis," *Computer-Aided Design of Integrated Circuits and Systems, IEEE Transactions on*, vol. 26, no. 1, pp. 86–99, Jan 2007.

[11] J.-H. Park, S. Shin, J. Christofferson, A. Shakouri, and S.-M. Kang, "Experimental validation of the power blurring method," in *Semiconductor Thermal Measurement and Management Symposium, 2010. SEMI-THERM 2010. 26th Annual IEEE*, Feb 2010, pp. 240–244.

[12] A. Vincenzi, A. Sridhar, M. Ruggiero, and D. Atienza, "Fast thermal simulation of 2D/3D integrated circuits exploiting neural networks and GPUfs," in *Proceedings of the 17th IEEE/ACM International Symposium on Low-power Electronics and Design*, ser. ISLPED '11.   Piscataway, NJ, USA: IEEE Press, 2011, pp. 151–156.

[13] Q. Xie, M. J. Dousti, and M. Pedram, "Therminator: A thermal simulator for smartphones producing accurate chip and skin temperature maps," in *Proceedings of the 2014 International Symposium on Low Power Electronics and Design*, ser. ISLPED '14.   New York, NY, USA: ACM, 2014, pp. 117–122.

[14] Z. Luo, H. Cho, X. Luo, and K. il Cho, "System thermal analysis for mobile phone," *Applied Thermal Engineering*, vol. 28, no. 14?15, pp. 1889 – 1895, 2008.

[15] S. Gurrum, D. Edwards, T. Marchand-Golder, J. Akiyama, S. Yokoya, J. Drouard, and F. Dahan, "Generic thermal analysis for phone and tablet systems," in *Electronic Components and Technology Conference (ECTC), 2012 IEEE 62nd*, May 2012, pp. 1488–1492.

[16] Y. Cengel and A. Ghajar, *Heat and Mass Transfer: Fundamentals and Applications*.   McGraw-Hill Education, 2010.

[17] A. Cohen, F. Finkelstein, A. Mendelson, R. Ronen, and D. Rudoy, "On estimating optimal performance of CPU dynamic thermal management," *IEEE Computer Architecture Letters*, vol. 2, no. 1, p. 6, 2003.

[18] S. Zhang and K. S. Chatha, "Approximation algorithm for the temperature-aware scheduling problem," in *Proceedings of the 2007 IEEE/ACM International Conference on Computer-aided Design*, ser. ICCAD '07.   Piscataway, NJ, USA: IEEE Press, 2007, pp. 281–288.

[19] P. Chaparro, J. Gonzalez, G. Magklis, Q. Cai, and A. Gonzalez, "Understanding the thermal implications of multi-core architectures," *IEEE Transactions on Parallel and Distributed Systems*, vol. 18, no. 8, pp. 1055–1065, 2007.

[20] T. Heath, A. P. Centeno, P. George, L. E. Ramos, Y. Jaluria, and R. Bianchini, "Mercury and freon: temperature emulation and management for server systems." in *ASPLOS*.   ACM, 2006, pp. 106–116.

[21] R. Jayaseelan and T. Mitra, "Temperature aware task sequencing and voltage scaling," in *Proceedings of the 2008 IEEE/ACM International Conference on Computer-Aided Design*, ser. ICCAD '08.   Piscataway, NJ, USA: IEEE Press, 2008, pp. 618–623.

[22] D. Forte and A. Srivastava, "Energy- and thermal-aware video coding via encoder/decoder workload balancing," *ACM Trans. Embed. Comput. Syst.*, vol. 12, no. 2s, pp. 96:1–96:26, May 2013. [Online]. Available: http://doi.acm.org/10.1145/2465787.2465798

[23] A. Weissel and F. Bellosa, "Dynamic thermal management for distributed systems," in *Proceedings of the First Workshop on Temperatur-Aware Computer Systems (TACS'04)*, Munich, Germany, Jun. 2004.

[24] U. Besson, "Cooling and warming laws: an exact analytical solution," *European Journal of Physics*, vol. 31, no. 5, pp. 1107–1121, 2010.

[25] C. T. O'Sullivan, "Newton's law of cooling – a critical assessment," *American Journal of Physics*, vol. 58, no. 10, pp. 956–960, Oct. 1990.